Physics Faculty Publications   Physics

Occupied Surface-State Bands of Bi(1×1) Overlayers on an InAs(110) Surface Grown by Molecular-Beam Epitaxy

D. N. McIlroy
University of Rhode Island

David R. Heskett
University of Rhode Island, dheskett@uri.edu

D. M. Swanston

A. B. McLean

R. Ludeke

See next page for additional authors

Occupied Surface-State Bands of Bi(1×1) Overlayers on an InAs(110) Surface Grown by Molecular-Beam Epitaxy

Authors

D. N. McIlroy, David R. Heskett, D. M. Swanston, A. B. McLean, R. Ludeke, H. Munekata, M. Prietsch, and N. J. DiNardo

Occupied surface-state bands of Bi(1 × 1) overlayers on an InAs(110) surface grown by molecular-beam epitaxy

D. N. McIlroy and D. Heskett

Department of Physics, University of Rhode Island, Kingston, Rhode Island 02881

D. M. Swanston and A. B. McLean

Department of Physics, Queen's University, Kingston, Ontario, Canada K7L 3N6

R. Ludeke, H. Munekata, and M. Prietsch*

IBM Thomas J. Watson Research Center, P.O. Box 218, Yorktown Heights, New York 10598

N. J. DiNardo

Department of Physics and Atmospheric Science, Drexel University, Philadelphia, Pennsylvania 19104

The ordered $p(1\times1)$ monolayer phase of Bi on InAs(110) has been studied with the technique of angle-resolved ultraviolet photoemission spectroscopy. Three Bi-induced surface-state bands (S', S'', and S''') have been observed. Their respective band dispersions have been mapped along the high-symmetry lines of the surface Brillouin zone. The upper two bands, S' and S'', appear to be degenerate across most of the surface Brillouin zone except along the $\bar{\Gamma}$-$\bar{X}'$ symmetry line. The bandwidths of the Bi-induced states of Bi/InAs(110) are significantly narrower than that of Bi/GaAs(110) or Sb/GaAs(110). The polarization of these surface-state bands has been measured and compared to predictions of current theoretical models for Sb/GaAs(110).

I. INTRODUCTION

The main motivation for studying group-V semimetals on the (110) surface of compound semiconductors is that these systems have been shown to form atomically abrupt epitaxial interfaces free of alloying.[1-5] While significant theoretical and experimental work has been performed on group-V semimetals on III-V semiconductors, the majority have focused on Sb/GaAs(110),[6-13] where the Sb overlayer forms an epitaxially ordered $p(1\times1)$ structure for monolayer (ML) coverages.[1,2] This epitaxial ordering enables modeling of this system beyond a simple jellium metal picture of the overlayer, i.e., structural effects can now be considered. A number of theoretical models have been proposed for Sb on GaAs(110), and other III-V(110) semiconductor surfaces, to relate the effects of overlayer geometries to the electronic band structures.[6-9]

Due to the favorable structure of Sb/GaAs(110), attention has turned to additional group-V semimetals on III-V(110) semiconductors, most notably Bi/GaAs(110). The covalent radii of Bi are approximately 4% larger than those of Sb. The ratio of the Bi bulk lattice constant to GaAs(110) is 0.84, while that of Sb relative to GaAs(110) is 0.80. Like Sb, Bi has been shown to form an atomically abrupt, epitaxially ordered, $p(1\times1)$ structure on GaAs(110) for monolayer coverages, but with lattice dislocations occurring every six unit cells (every 12 Bi adatoms) along the Bi chains.[14,3] These dislocations have been attributed to strain induced in the Bi chains resulting from poor lattice matching between Bi and the GaAs(110) substrate. If we stipulate that Sb/GaAs(110)

represents a well-matched system, then an epitaxial overlayer of Bi on GaAs(110) will be under compression. A recent angle-resolved ultraviolet photoemission spectroscopy (ARUPS) experiment of Bi/GaAs(110) by McLean *et al.*[15] observed larger bandwidths for the Bi-induced surface-state bands than for corresponding bands of Sb/GaAs(110).[12] They attributed these larger bandwidths to either increased interaction between neighboring Bi atoms along the overlayer chains, or substrate mediated interactions. This enhancement in interaction may be the direct result of strain within the Bi overlayer.

In addition, the polarization of the corresponding surface states of Sb/GaAs(110) (Ref. 12) and Bi/GaAs(110) (Ref. 15) were observed to be quite different. This raises questions as to the universality of the epitaxially continued layer structure (ECLS) for group-V elements on compound (110) semiconductors [Fig. 1(c)]. La Femina, Duke, and Mailhiot[9] have investigated a competing model in which the element-V adatoms form zigzag chains, like the ECLS model, but with the chains registered directly above the semiconductor substrate chains rather than above and between them. This model, depicted in Fig. 1(d), is referred to as the epitaxially on top structure (EOTS). At this time, it is unclear as to which bonding scheme, ECLS or EOTS, is correct. Even with the extensive studies of Sb and Bi/GaAs(110), a number of interesting questions still remain unanswered.

The purpose of the present set of experiments is to obtain additional information on the effects of the lattice match between the overlayer and the substrate on the electronic band structure. Considering the strain in the Bi/GaAs(110) system, the cubic lattice constant of
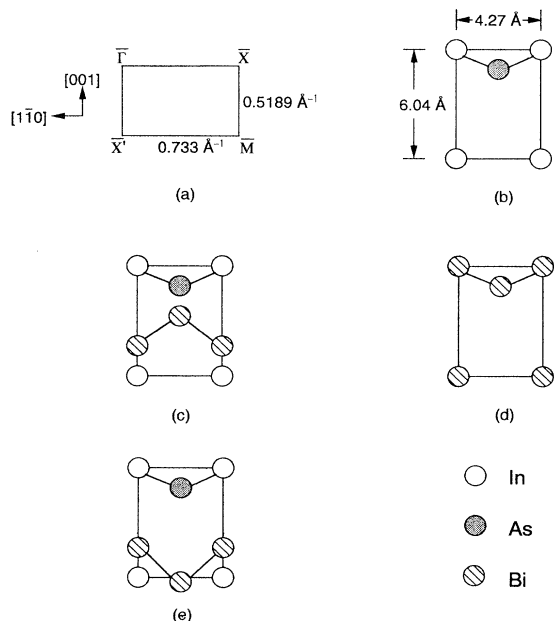
FIG. 1. (a) The surface Brillouin zone of InAs(110). (b) The real-space unit cell of InAs(110). (c)–(e) are three of the possible structures for Bi on InAs(110). (c) The epitaxially continued layer structure (ECLS). (d) The epitaxially on top structure (EOTS). (e) The p^3 structure.

InAs(110) (6.036 Å) is approximately 7% larger than GaAs(110) (5.65 Å). The larger unit-cell size of InAs(110), with respect to GaAs(110), should better accommodate Bi. Low-energy-electron-diffraction (LEED) and scanning-tunneling-microscopy (STM) studies of Bi/InAs(110) (Refs. 15 and 16) have in fact shown that the dislocations observed for Bi/GaAs(110) are eliminated. This is most likely a consequence of the better lattice match between Bi and the InAs substrate. Comparisons between Sb/GaAs(110), Bi/GaAs(110), and Bi/InAs(110) should assist in identifying trends, which arise from variations in the degree of the lattice match between the overlayer and the substrate.

II. EXPERIMENTAL SETUP

The experiment was performed on beamline U12B at the National Synchrotron Light Source (NSLS), Brookhaven National Laboratory. The radiation was dispersed using a toroidal grating monochromator, which has been described elsewhere.[17] The surfaces were prepared, and data acquired, in a magnetically shielded UHV chamber with LEED and Ar-ion sputtering capabilities. A chamber base pressure of 1×10^{-10} Torr was achieved. The chamber was equipped with an angle-resolved hemispherical electrostatic energy analyzer[18] with an angle of acceptance of $\pm 2°$. The overall energy resolution was approximately 200 meV. The sample was oriented such that the **A** vector of the incident photons was parallel to the $[1\bar{1}0]$ direction of the substrate [Fig. 1(a)].

The sample consisted of a thick molecular-beam-epitaxial (MBE)-grown InAs(110) film on a GaAs(110) substrate. InAs is an intrinsically doped n-type semiconductor and, consequently, no additional doping was introduced during the MBE growth process. The InAs(110) sample was mounted on Ta foil, which was supported by two Ta wires. Current was passed through the Ta wires to resistively heat the sample. The temperature was monitored with a thermocouple attached to the Ta foil backing plate near the sample. The backing plate was mounted on a manipulator with rotational capabilities about two independent axes.

The sample was cleaned by Ar-ion sputtering followed by a 10–15-min anneal at 400 °C. Photoemission spectra acquired at normal emission for our clean MBE-grown InAs(110) sample[19] compared favorably to previous photoemission spectra by Williams *et al.*[20] of a clean cleaved single crystal of InAs(110), demonstrating the integrity of our MBE-grown sample. Subsequent sputtering and annealing of the MBE-grown InAs(110) sample resulted in reproducible valence spectra, which verified our ability to generate a clean, atomically ordered, substrate.

Bi was evaporated onto the clean InAs substrate from a boron-nitride effusion cell. During evaporation, the chamber pressure did not exceed 3×10^{-10} Torr. After deposition, the sample was subsequently annealed at 130 °C for 5 min. The Bi thickness was determined from timed exposures to the Bi evaporant beam. Deposition rates were established with a crystal-thickness monitor. We estimate the accuracy of the overlayer to within 25%, with a reproducibility of approximately 10%. One monolayer of Bi is defined as two adatoms per unit cell of the InAs(110) substrate $(7.75 \times 10^{14} \, cm^2)$. We have assumed a linear relationship between the sticking coefficient of Bi to the sample and the thickness monitor.

III. RESULTS

A. Determination of Bi coverage

STM images have shown that Bi deposited on InAs(110) follows the Stranski-Krastanov (SK) growth mode where the first ML grows in a laminar fashion with subsequent layers growing in islands.[16] It is important to determine when the first monolayer is complete, since the electronic structure of a laminar overlayer relative to one possessing an excess of three-dimensional islands may be dramatically different. The In $4d$ and Bi $5d$ core level intensities were monitored in order to determine when the formation of the first ML was completed.

Figure 2 shows plots of the normalized areas of both the In $4d$ and Bi $5d$ cores vs Bi coverage. The In $4d$ core-level photoemission intensities are normalized to the clean substrate and the Bi core-level intensities to the core-level area corresponding to four ML. We see the typical attenuation of the intensity of the In core level associated with the deposition of an overlayer. As observed with other group-V semimetals on compound semiconductors,[21] attenuation of the In core level is linear up to the first ML of Bi (laminar growth) followed by a break, which is associated with the completion of the first ML
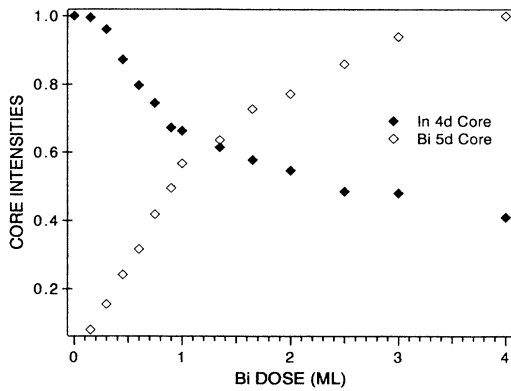
FIG. 2. The integrated intensities of the In $4d$ and Bi $5d$ core levels as a function of Bi coverage. The In $4d$ core-level intensities have been normalized to the clean substrate and the Bi $5d$ core-level intensities to the four-monolayer coverage.

and the onset of multilayer growth.[22] As expected, the Bi $5d$ core-level intensity increases linearly, followed by a break in the curve, signifying the completion of the first ML. Both breaks in the core-level intensity curves coincide. By using these breaks to calibrate the thickness monitor, we were able to ensure the repeatability of the dosing process.

B. Bi-induced surface states

In Fig. 3 we present angle-resolved photoemission energy-distribution curves of a dosing sequence taken at
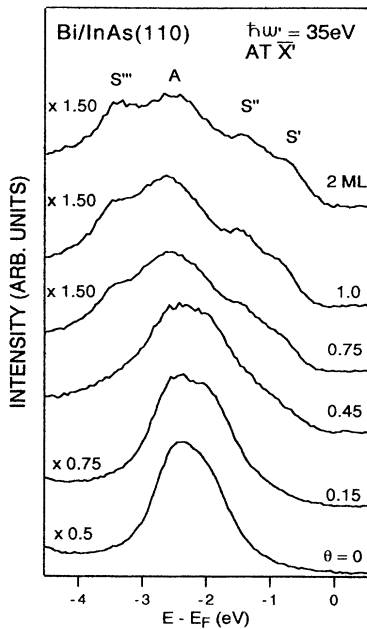

FIG. 3. Angle-resolved photoemission spectra of the valence band at $\overline{X}'$ for clean InAs(110) and for Bi coverages up to two monolayers. Three new surface states are located at -0.89 eV (S'), -1.39 eV (S''), and -3.49 eV (S'''), relative to the sample Fermi level.

the $\overline{X}'$ point of the surface Brillouin zone with a photon energy of 35 eV. This is the only region of the surface Brillouin zone where all three of the Bi-induced surface-state bands are simultaneously observed. The spectra have been shifted to account for band bending associated with the deposition of Bi, as determined from shifts in the In $4d$ core level. All energy-distribution curves are referenced to the Fermi level of the sample holder. The Fermi level was established from photoemission spectra of the sample holder at normal emission assuming that no potential existed between the sample and the holder. The lower energy distribution curve is that of the clean InAs substrate. At a coverage of approximately 0.45 ML three new Bi-induced features begin to emerge. Upon completion of the first ML, these new features can be identified on either side of what appears to be a residual substrate feature (labeled A in Fig. 3). Following an earlier convention,[6,8] we have labeled these Bi-induced surface states, from lower to higher binding energy, S' (-0.89 eV), S'' (-1.39 eV), and S''' (-3.49 eV), respectively. These states are fully developed upon completion of the first monolayer. For coverages exceeding 1 ML, these features begin to broaden, which is indicative of overlayer disordering associated with the formation of the second ML, i.e., the onset of three-dimensional (3D) Bi island formation.[13] Three overlayer-induced surface-state bands have also been observed for both Sb/GaAs(110) (Ref. 12) and Bi/GaAs(110) (Ref. 15) at coverages of 1 ML.

Due to the two-dimensional nature of surface states, they should not disperse with changes in the energy of the incident photons at normal incidence. To ensure that S', S'', and S''' were indeed two-dimensional surface-state bands, photoemission spectra were taken at $\overline{X}'$ for incident photon energies ranging from 16–35 eV. While the intensities of the surface states varied with changes in the photon energy, their binding energies remained constant, establishing their two-dimensional nature.

Photoemission spectra were acquired along the high-symmetry lines of the surface reciprocal lattice. In this manner it was possible to map the two-dimensional band dispersion of the Bi-induced surface states. The parallel component of the wave vectors of the photoelectrons were calculated using the standard equation, $k_{\parallel} = (2mE/\hbar)^{1/2}\sin\theta$, where $k_{\parallel}$ is the parallel component of the photoelectron's wave vector, E is the kinetic energy of the electrons, m is the electron's mass, $\hbar$ is Planck's constant divided by 2π, and θ is the angle of emission of the photoelectrons with respect to the sample normal.

1. $\overline{\Gamma}$-$\overline{X}'$ symmetry line

As in the cases of Sb/GaAs(110) (Ref. 12) and Bi/GaAs(110) (Ref. 15), it is only along the $\overline{X}'$-$\overline{\Gamma}$ symmetry line of the second zone that the adsorbate-induced surface states S', S'', and S''' can simultaneously be observed. In Fig. 4 we present photoemission spectra acquired along the $\overline{X}'$-$\overline{\Gamma}_2$ symmetry line of the second surface Brillouin zone for one ML of Bi. At approximately two thirds of the way across the zone ($k_{\parallel}=0.893$ Å^{-1}), S'' appears to merge with S', forming a single peak. At the same time, both S''' and the substrate feature A
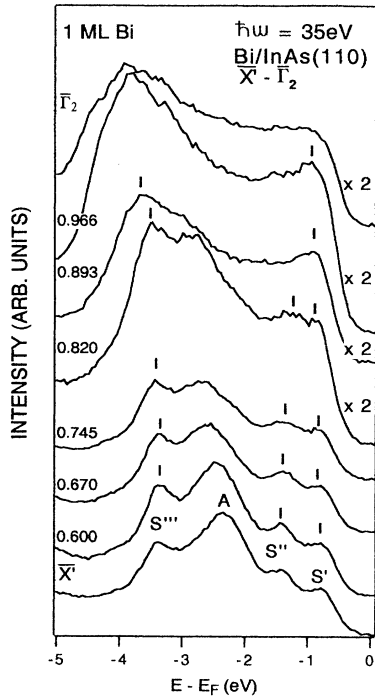
FIG. 4. Angle-resolved photoemission spectra of the valence band along the $\bar{X}'$-$\bar{\Gamma}_2$ symmetry line with a Bi coverage of one monolayer.
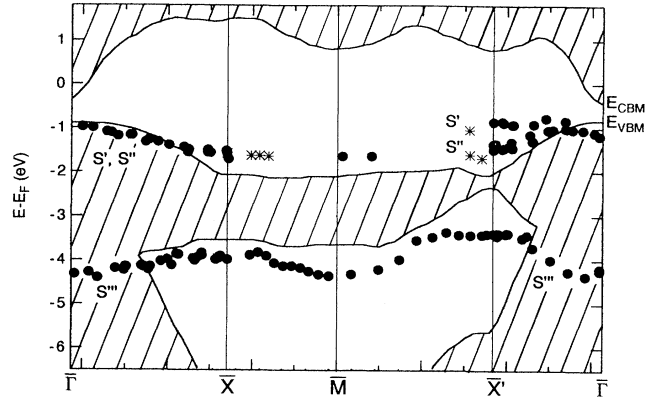

FIG. 5. The surface-state band dispersions referenced to the sample Fermi level of monolayer coverages of Bi on InAs(110). The symbols are the experimentally determined dispersions for S', S'', S'''. Asterisks indicate when bands appeared as shoulders in the photoemission spectra. The hatched regions are the theoretical bulk band projections from Ref. 8 for clean InAs(110).

disperse to higher binding energies until they merge at $\bar{\Gamma}_2$. A comparison of Fig. 4 with Fig. 8 of Ref. 15 of Bi/GaAs(110) illustrates the remarkable similarities between the two systems with regard to the positions and dispersions of the Bi-induced states.

The measured dispersion of the three Bi-induced surface-state bands S', S'', and S''' along the high-symmetry lines of the surface Brillouin zone are presented in Fig. 5. The hatched areas are theoretical bulk band projections;[8] the two uppermost solid lines are the conduction-band minimum (E_{CBM}) and the valence-band maximum (E_{VBM}), respectively, referenced to the experimentally determined Fermi-level energy of the sample. The valence-band maximum for our sample was determined by acquiring photoemission spectra of the clean substrate at $\bar{\Gamma}$,[23] and was used as the reference point between the theoretical bulk-band projections and the measured band structure of the Bi-induced surface states. The two-dimensional Bi-induced surface-state bands are represented by symbols in Fig. 5. Photon energies of 22, 30, and 35 eV were used for the acquisition of the photoemission spectra. We found that the photoemission intensity of the Bi-induced surface states was significantly enhanced with a photon energy of 35 eV. Photon energies lower than 22 eV were observed to enhance photoemission from the substrate bands rather than the Bi-induced surface-state bands.

In Fig. 5 we see that S' and S'' are degenerate, or nearly degenerate, at $\bar{\Gamma}$, but quickly diverge from one another at the zone boundary as $\bar{X}'$ is approached, at which point they appear as distinct bands. The dispersion of the Bi-

induced surface-state bands are not as dramatic along this symmetry line, in comparison to other regions of the surface Brillouin zone.

2. $\bar{X}$-$\bar{M}$-$\bar{X}'$ symmetry lines

Due to the proximity in binding energy of S' and S'' to one another, and the strong InAs substrate feature (see Fig. 3), it is difficult to identify S' and S'' along the $\bar{X}$-$\bar{M}$ symmetry line of the surface Brillouin zone. Consequently, we have tentatively identified shoulders in the energy distribution curves as a single degenerate S'-S'' state along the $\bar{X}$-$\bar{M}$ symmetry line. These shoulders are represented by asterisks in Fig. 5.

On the other hand, it is possible to map S''' entirely along the $\bar{X}$-$\bar{M}$ symmetry line. In Fig. 5 we see that S''' disperses by 0.41 eV, while for Bi/GaAs(110) the observed bandwidth of S''' is 1.02 eV.[15] This reduction in the bandwidth of S''' of Bi/InAs(110) may be due to the higher degree of the lattice match between the overlayer and the substrate, which results in reduced orbital wave-function overlap, in comparison to Bi/GaAs(110). This will be explored in greater detail in the discussion.

As with the symmetry line $\bar{X}$-$\bar{M}$, we were only able to partially extract the dispersions of S' and S'' along the $\bar{M}$-$\bar{X}'$ symmetry line prior to their merging. Consequently, data points for S' and S'' are only designated as shoulders near $\bar{X}'$ in Fig. 5. As we map from $\bar{X}'$ towards $\bar{M}$, we see that S' disperses to higher binding energies until near the center of the zone S' and S'' merge. As $k_\parallel$ approaches $\bar{M}$, only a single band is observed, which is consistent with a degenerate, or near-degenerate, S'-S'' band along the $\bar{\Gamma}$-$\bar{M}$ symmetry line.

For $\bar{M}$-$\bar{X}'$, S''' disperses across the entire zone without overlapping with substrate bands. The measured bandwidth of S''' along the $\bar{M}$-$\bar{X}'$ symmetry line is 0.97 eV, which is significantly larger than for the $\bar{X}$-$\bar{M}$ symmetry

line. This is consistent with the association of S'''' with Bi-Bi intrachain bonds. The $\bar{M}$-$\bar{X}$' symmetry line corresponds to the $[1\bar{1}0]$ direction in reciprocal space, which in real space is the direction parallel to the Bi chains. It is along this direction that we expect the highest degree of hybridization between the constituents of the overlayer and therefore the greatest dispersion. On the other hand, the $\bar{X}$-$\bar{M}$ symmetry line corresponds to the $[00\bar{1}]$ direction, which in real space is perpendicular to the chains. Therefore, the interatomic spacing between the neighboring Bi adatoms is larger along this direction in comparison to the $[1\bar{1}0]$ direction. The net effect is smaller bandwidths as a result of the decreased hybridization of the electron orbitals between neighboring Bi adatoms.

3. $\bar{\Gamma}$-$\bar{X}$ symmetry line

Only two surface-state bands are observed along the $\bar{\Gamma}$-$\bar{X}$ symmetry line of the surface Brillouin zone. We have included the dispersions from the first and second zones, $\bar{\Gamma}$-$\bar{X}$ and $\bar{X}$-$\bar{\Gamma}_2$, respectively. As with the photoemission studies of Bi/GaAs(110),[15] the Bi-induced surface states are most often resolved by measuring in the second Brillouin zone. In Fig. 5 we see that S' mixes with the bulk bands, but as $k_\parallel$ approaches the $\bar{X}$ point of the surface Brillouin zone S' disperses into the semiconductor gap. It is our belief that this band is a degenerate combination of S' and S''. In Fig. 5 we see that S''' disperses very little along this symmetry line.

C. Polarization studies

We have also studied the intensity of the Bi-induced surface states as a function of the incidence angle of the light. Because the synchrotron light is linearly polarized, changing the angle of incidence changes the projection of the $\mathbf{A}$ vector into the substrate. In the dipole approximation, the transition probability is proportional to $|\langle f|\mathbf{A}\cdot\mathbf{p}|i\rangle|^2$, where $\mathbf{p}$ is the momentum operator and $|i\rangle$ and $\langle f|$ are the initial- and final-state eigenvectors, respectively. Therefore, if the initial state has p-like symmetry, the photoemission transition probability is maximized when the projection of the $\mathbf{A}$ vector lies along the p orbital and is proportional to $\cos^2(\theta)$, where θ is the angle between $\mathbf{A}$ and the p orbital. We define a state deriving primarily from a p orbital perpendicular to the substrate as possessing a p_z-like dependence. Conversely, we define a state deriving primarily from p orbitals parallel to the substrate as possessing a p_{xy}-like dependence.

In Fig. 6 we present the energy distribution curves of the polarization studies acquired at the $\bar{X}$' point of the surface Brillouin zone with a photon energy of 35 eV for one ML of Bi. As we previously mentioned, it is at the $\bar{X}$' point of the surface Brillouin zone that all three of the Bi-induced surface-state bands are individually resolved. From the energy distribution curves of Fig. 6, we see that the intensity of S' decreases as the angle of incidence is increased, an indication of p_{xy}-like dependence. The persistence of S' at large incidence angles, e.g., $\theta_i = 70°$ (topmost curve of Fig. 6), suggests that S' is not strictly p_{xy}
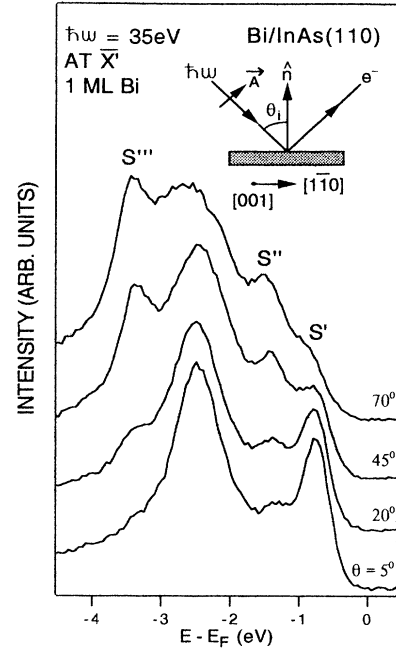

FIG. 6. Angle-resolved photoemission spectra taken at the $\bar{X}$' point of the surface Brillouin zone with varying photon incident angles. The experimental geometry is illustrated in the upper right-hand corner of the figure.

like but, in addition, possesses a smaller p_z-like dependence.

On the other hand, S'' appears to be oppositely polarized with respect to S'. From Fig. 6 we see that the intensity of S'' increases as the angle of incidence increases. This suggests that S'' is primarily p_z-like dependent. For small angles of incidence, e.g., $\theta_i = 5°$, remnants of S'' are still present, indicating a smaller p_{xy}-like dependence.

The polarization dependence of S''' is different from the polarization dependence of both S' and S''. While the polarization dependencies of S' and S'' are in the plane of the substrate, as well as perpendicular to the substrate, this is not the case for S'''. In Fig. 6 we see that S''' is very pronounced for large angles of incidence and all but disappears for an incidence angle of 5°. Consequently, we can conclude that the polarization dependency of S''' is almost exclusively p_z-like.

The magnitude of the p_{xy} polarization dependence of the Bi-induced surface states can be determined by fitting their normalized intensities to the function $\sin^2(\theta_i) + \beta\cos^2(\theta_i)$, where β is an adjustable parameter, which represents the ratio of p_{xy} polarization to p_z polarization,

TABLE I. The ratio of the p_{xy} to p_z-like polarization (β) of the Bi-induced surface-state bands.

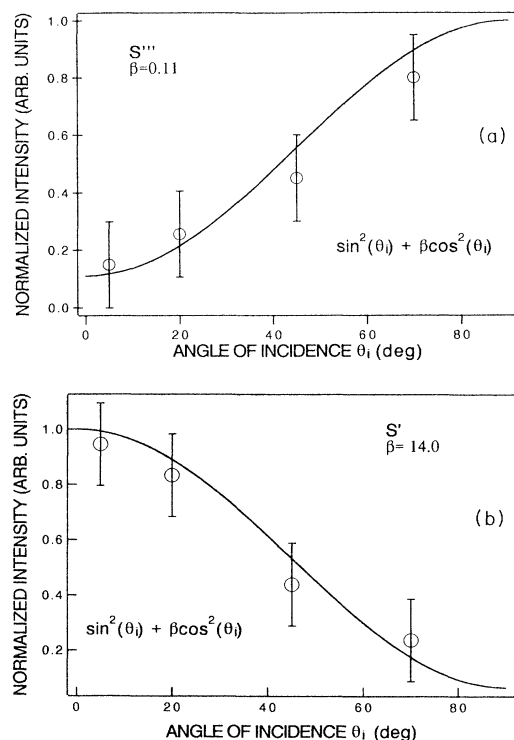|	Bi/InAs(110)	Bi/GaAs(110) (Ref. 15)
S'	14.0±0.10	0.15±0.05
S''	0.55±0.10	0.15±0.05
S'''	0.11±0.10	0.25±0.05

FIG. 7. The normalized intensities of Bi-induced states (at $\bar{X}'$) as a function of photon incidence angle θ_i. The open symbols are the observed intensities and the solid lines are curves fitted to the data with the trial function of the form $\sin^2(\theta_i)+\beta\cos^2(\theta_i)$, where β is the ratio of p_{xy} polarization to p_z polarization. (a) The observed polarization dependence of S'''. (b) The observed polarization dependence of S'.

and θ_i is the angle of incidence of the photons. The results of the fits, as well as the normalized intensities of S' and S''', have been plotted against the photon incidence angle (θ_i) and are presented in Fig. 7. A summary of the β parameters for the surface states of Bi/InAs, as well as Bi/GaAs, are summarized in Table I. A large value for β (>1) is indicative of a surface state with a strong p_{xy} polarization dependence.

IV. DISCUSSION

While the ECLS model is the accepted structure for Sb/GaAs(110), LaFemina, Duke, and Mailhiot[9] have proposed the epitaxially on top structure as an alternative model for group-V elements on III-V(110) semiconductors [see Fig. 1(d)]. In the EOTS model, the intrachain bond lengths of the overlayer are held constant, while intrachain bond angles are allowed to vary. LaFemina, Duke, and Mailhiot have arrived at a critical intrachain bond angle of $\theta < 90°$, which would favor EOTS over ECLS.

In addition to ECLS and EOTS, an alternative model utilizing a "p^3" bonding scheme has been proposed by Skeath *et al.*[7] [see Fig. 1(e)]. While the ECLS model was found to demonstrate the best agreement with STM im-

ages of Sb/GaAs(110) by Mårtensson and Feenstra,[24] the p^3 model was also found to be acceptable. In the p^3 model, the overlayer adatoms only bond to the cation of the substrate, leaving the other adatom of the unit cell bound only to adjacent overlayer adatoms. In both the ECLS and EOTS models, one of the two adatoms in the unit cell bonds to the cation and the other bonds to the anion of the substrate. While the orbital nature of the bonds for the p^3 and the EOTS models are similar, they differ in the effects of the overlayer on the geometry of the substrate. In the EOTS model the substrate unrelaxes, while for the p^3 model the substrate remains fully relaxed.

Recent STM studies of Bi/InAs(110) by Samsavar, Prietsch, and Ludeke[16] have found that Bi forms chains above, or slightly shifted from directly above, the InAs substrate chains. If the Bi overlayer forms an epitaxial on top structure on InAs(110), this would be unexpected, since the ratio of the Bi bulk lattice constant to the (110) surface of InAs (0.787) is comparable to that of Sb to GaAs(110) (0.798). Subsequently, we do not expect the overlayer intrachain bond angles of Bi/InAs(110) to fall within the range necessary for the promotion of EOTS. This may indicate that a driving mechanisms other than overlayer-substrate lattice-mismatch-induced strain is dictating the overlayer structure, as suggested by LaFemina, Duke, and Mailhiot[9]. The similarities in the structures of Sb and Bi on GaAs(110), combined with the unexpected structure of Bi/InAs(110), suggests that the substrate may play a larger role in dictating the overlayer structure than the overlayer material (Sb or Bi). It will be interesting to examine the electronic and overlayer structures of Sb/InAs(110) in order to compare with Bi/InAs(110).

At this time the theoretical work for the above models of Sb on the compound semiconductor (110) surfaces have only been expanded to include Bi/GaAs(110).[25] Consequently, we have only compared the results of our angle-resolved photoemission study of Bi/InAs(110) with the theoretical models of Sb on compound semiconductors. In addition, we will also compare our results with earlier photoemission studies of Sb/GaAs(110) and Bi/GaAs(110).

A. Band dispersion

As in the case of Sb/GaAs(110) (Ref. 12) and Bi/GaAs(110) (Ref. 15), three new adsorbate-induced features have been identified for Bi/InAs(110). This is not surprising in light of the fact that all three systems consist of monolayer coverages of group-V elements, which exhibit epitaxially ordered $p(1\times1)$ structures on the (110) surfaces of III-V semiconductors. The main difference between these systems, electronic differences aside, is the degree of lattice matching between the overlayers and the substrates. In terms of electronic states, for Sb/GaAs(110) (Ref. 12) and Bi/GaAs(110) (Ref. 15), the uppermost occupied surface-state band S' is a gap state located above the valence-band maximum (VBM) across the entire surface Brillouin zone. For Bi/InAs(110) this is not the case. Upon examination of Fig. 5, we see that S' of Bi/InAs(110) overlaps with the

bulk bands in the $\bar{\Gamma}$-$\bar{X}$ and $\bar{\Gamma}$-$\bar{X}'$ regions of the surface Brillouin zone.

Upon comparing the dispersions of S', S'', and S''' across the surface Brillouin zone for Sb/GaAs(110),[12] Bi/GaAs(110),[15] and Bi/InAs(110), greater similarities in the dispersions of the surface-state bands are observed between Sb/GaAs(110) and Bi/GaAs(110) than between Bi/GaAs(110) and Bi/InAs(110). In Table II we present a summary of the bandwidths of the upper three surface states for Sb/GaAs(110), Bi/GaAs(110), and Bi/InAs(110) for the $\bar{\Gamma}$-$\bar{X}$ symmetry line. S' of Bi/InAs(110) is fairly flat along the $\bar{\Gamma}$-$\bar{X}$ symmetry line, when compared to Sb/GaAs(110), which is interesting, since the lattice match between the overlayer and the substrate for the two systems is nearly identical. For Sb/GaAs(110) and Bi/GaAs(110) the bandwidths of S' along the $\bar{\Gamma}$-$\bar{X}$ symmetry line are comparable. The bandwidth of S' along the $\bar{\Gamma}$-$\bar{X}'$ symmetry line varies significantly from system to system (see Table III).

The bandwidths of the three surface-state bands of Bi/InAs(110), on average, are significantly narrower in comparison to the corresponding bands of Bi/GaAs(110).[15] This is most likely due to a combination of effects. The first is the larger lattice constant of InAs relative to GaAs, which in turn could increase the intrachain bond angles between neighboring adatoms. A second possibility is an expansion of the Bi chains along the [1$\bar{1}$0] direction, as a consequence of the overlayer structure observed by STM of Bi/InAs(110),[16] which could increase bond lengths as well as bond angles. The combined effect would be a reduction in the overlap of the electron wave functions between neighboring Bi adatoms. This will result in the narrowing of the bandwidths of the surface-state bands of the Bi overlayer of Bi/InAs(110), in comparison to the corresponding bands of Bi/GaAs(110).[15] At the same time, the similarities between the surface-state band structures of Sb/GaAs(110) (Ref. 12) and Bi/GaAs(110) (Ref. 15) combined with the differences between Bi/InAs(110) and these systems, suggests that the electronic properties of the substrate has a greater effect on the electronic band structure of these systems than previously believed, which in turn affects the overlayer structure.

In Fig. 5 only two surface-state bands are observed in the $\bar{\Gamma}$-$\bar{X}$ region of the surface Brillouin zone. We have tentatively assigned the uppermost band as a degenerate pairing of S' and S'' based on the polarization studies. It is along the $\bar{M}$-$\bar{X}'$ symmetry line that S' and S'' appear to merge. In their calculations of Sb/GaAs(110), Mailhiot, Duke, and Chadi[8] initially determined the dispersion of the surface-state bands for isolated chains of Sb. They

TABLE II. Bandwidths of the surface-state bands along the $\bar{\Gamma}$-$\bar{X}$ symmetry line.

	Bi/InAs(110)	Bi/GaAs(110) (Ref. 15)	Sb/GaAs(110) (Ref. 12)
S'	0.60 eV	0.98 eV	1.05 eV
S''	0.60 eV	1.55 eV	
S'''	0.33 eV	1.03 eV	

TABLE III. Bandwidths of the surface-state bands along the $\bar{\Gamma}$-$\bar{X}'$ symmetry line.

	Bi/InAs(110)	Bi/GaAs(110) (Ref. 15)	Sb/GaAs(110) (Ref. 12)
S'	0.23 eV	0.83 eV	0.50 eV
S''	0.32 eV	0.40 eV	
S'''	0.79 eV	1.40 eV	

found that the upper two bands of these chains (S_5 and S_6) are degenerate, and not until the Sb chains are brought into contact with the semiconductor surface is the degeneracy lifted by the surface potential. The apparent degeneracy of S' and S'' of Bi/InAs(110) may be indicative of the interaction between the Bi chains and the substrate.

McLean et al.[15] have observed a feature at a higher binding energy in the $\bar{\Gamma}$-$\bar{X}$ region of the surface Brillouin zone of Bi/GaAs(110), which they have attributed to the remnants of an As-derived dangling bond (A_5). Consequently, only one Bi-induced feature (S') is identified, as in the case of Bi/InAs(110). On the other hand, Mårtensson et al.[12] observed a second surface feature of Sb/GaAs(110) in this region of the surface Brillouin zone, which they identified as S_5. It appears from Fig. 9 of Ref. 15 that the surface-state bands S' and S'' of Bi/GaAs(110) may also be degenerate along most of the $\bar{\Gamma}$-$\bar{X}$ symmetry line of the surface Brillouin zone. If this is the case, it may well be a consequence of having a Bi overlayer rather than Sb.

B. Polarization studies of the Bi-induced surface-state bands

The polarization dependence of the surface-state bands of Bi/InAs(110) provides additional information about the bonding of the overlayer to the substrate. The relatively good agreement between our results for the band structure of Bi/InAs(110) and the theoretically determined band structure of Sb/InAs(110) (Ref. 8) has enabled us to make a one-to-one identification of the Bi-induced surface states with the corresponding states of the theoretical calculation.

In Table IV we have summarized *our interpretation* of the polarization dependencies of the surface-state bands for a number of theoretical models of Sb/GaAs(110), as well as the experimental results of Bi/InAs(110), Bi/GaAs(110),[15] and Sb/GaAs(110).[12] The polarization dependence of the surface-state bands, both experimentally and theoretically, are not expected to be exclusively p_z-like or p_{xy}-like. Consequently, we have defined a secondary polarization dependence as a component of polarization dependence which is small in comparison to the primary polarization dependence of a surface-state band. The secondary polarization dependence of the surface-state bands of the theoretical models of Sb/III-V(110) semiconductors are in parentheses in Table IV.

There is only marginal agreement between the polarization of the surface-state bands of Bi/InAs(110) and the models presented in Table IV. While the polarization dependence of the Bi-induced states of Bi/InAs(110) are

TABLE IV. Observed and predicted polarization of the absorbate-induced surface-state bands.

Surface state	ECLS (Ref. 6)	ECLS (Ref. 8)	EOTS (Ref. 9)	p^3 (Ref. 7)	Bi/InAs(110)	Bi/GaAs(110) (Ref. 15)	Sb/GaAs(110) (Ref. 12)
S'	p_z	p_z (p_{xy})	p_z (p_{xy})	p_z (p_{xy})	p_{xy}	p_z	p_z
S''	p_z	p_z (p_{xy})	p_z (p_{xy})	p_z (p_{xy})	p_z	p_z	p_z
S'''	p_z (p_{xy})	p_{xy}	p_{xy}	p_z (p_{xy})	p_z	p_z	p_{xy}

very well defined, it is difficult to make a comparison with the theoretical models, since they do not explicitly address in detail the issue of the polarization dependence of the adsorbate-induced surface-state bands.

From Table I we see that the polarization dependence of the surface-state bands of Bi/InAs(110) and Bi/GaAs(110) are substantially different. Only in the case of S''', which exhibits a strong p_z-like dependence, do we observe similarities between these two systems. For Bi/InAs(110), S' exhibits a strong p_{xy}-like dependence, while the corresponding state of Bi/GaAs(110) is p_z-like. S'' is strongly p_z-like in both systems, but a much larger p_{xy}-like dependence is observed for Bi/InAs(110).

The difference in the extent of the p_{xy}-like dependence of S'' between Bi/InAs(110) and Bi/GaAs(110) may be a consequence of the alignments of the samples relative to the **A** vector of the light source. For Bi/InAs(110), the sample was oriented such that the **A**-vector of the incident photons was parallel to the [1$\bar{1}$0] direction of the substrate. This orientation would preferentially enhance the photoemission process from surface-state bands with p_{xy}-like dependence deriving from bonds along the direction of the Bi chains. For Bi/GaAs(110), the **A** vector of the incident photons was parallel to the [001] direction of the substrate. This orientation would preferentially enhance the photoemission process from surface-state bands with p_{xy}-like dependence deriving from bonds perpendicular to the direction of the Bi chains.

From Table IV we see that the polarization dependence of S' and S''' of Bi/InAs(110) are the reverse of the corresponding states of Sb/GaAs(110). Strain arguments proposed to explain the differences between the polarization dependencies of the surface-state bands of Bi/InAs(110) and Sb/GaAs(110) are not justified in this case. Alternatively, the electronic environments of Bi/InAs(110) and Sb/GaAs(110) may be sufficiently different that one bonding scheme may be favored over another. This could be the case between Bi/InAs(110) and Bi/GaAs(110).

The degree of diversity between the polarization dependence of the adsorbate-induced surface-state bands of Bi/InAs(110), Bi/GaAs(110), and Sb/GaAs(110) are rather surprising. These results raise questions about the similarities of these systems. Regardless of the cause of the dissimilarities between the polarization dependencies of the adsorbate-induced surface state bands of Bi/InAs(110), Bi/GaAs(110), and Sb/GaAs(110), these results should provide useful information and insight towards arriving at a better understanding of group-V elements on the (110) surfaces of compound semiconductors.

V. CONCLUSION

In summary, we have probed the occupied electronic surface-state band structure of the InAs(110)-p(1×1)-Bi system with the technique of angle-resolved ultraviolet photoemission spectroscopy. We chose to study this system in an effort to further our understanding of the effects of overlayer-substrate lattice matching on the electronic and structural properties of group-V elements on III-V(110) semiconductors. Similar to Sb/GaAs(110) (Ref. 12) and Bi/GaAs(110) (Ref. 15), three new surface-state bands have been identified. Comparisons between these three systems revealed that the bandwidths of the absorbate-induced surface states of Sb/GaAs(110) (Ref. 12) and Bi/GaAs(110) (Ref. 15) are comparable, while the bandwidths of Bi/InAs(110) are relatively flat with respect to the other two systems. A recent STM study of Bi/InAs(110) (Ref. 16) suggests that the Bi overlayer chains may be registered above the InAs substrate chains rather than above and between, in contrast to Sb/GaAs(110) and Bi/GaAs(110). It is our opinion that this geometry may allow the Bi chains to expand along the [1$\bar{1}$0] direction. This results in a reduction of the wave-function overlap between neighboring Bi adatoms within the overlayer chains, which in turn reduces the bandwidths of the surface-state bands.

The predictions by the ECLS, EOTS, and p^3 models of the polarization of the surface-state bands of Sb on the (110) surfaces of III-V semiconductors are all in partial agreement with the results of the polarization studies of Bi/InAs(110). Since these theoretical studies do not address in detail the question of the polarization dependence of the adsorbate-induced surface-state bands, we are unable to utilize our results of the polarization dependence studies of the surface-state bands of Bi/InAs(110) towards conclusively determining the overlayer structure. However, differences between the polarization dependence of the surface-state bands of Bi/InAs(110), Bi/GaAs(110),[15] and, in particular, with Sb/GaAs(110),[12] combined with the STM results, are indicative of the significant differences between these systems and raise new questions about the complexity of group-V elements on the (110) surfaces of compound semiconductors.

ACKNOWLEDGMENTS

*Permanent address: Institut fur Atom- und Festkorperphysik, Freie Universitat Berlin, D-1000, Berlin 33, Germany.

[1] C. B. Duke, A. Paton, W. K. Ford, A. Kahn, and J. Carelli, Phys. Rev. B **26**, 803 (1982).

[2] P. Mårtensson and R. M. Feenstra, Phys. Rev. B **39**, 7744 (1989).

[3] A. B. McLean, R. M. Feenstra, A. Taleb-Ibrahimi, and R. Ludeke, Phys. Rev. B **39**, 12 925 (1989).

[4] T. Guo, R. E. Atkinson, and W. K. Ford, Phys. Rev. B **41**, 5138 (1990).

[5] J. F. McGilp and A. B. McLean, J. Phys. C **21**, 807 (1988).

[6] C. M. Bertoni, C. Calandra, F. Manghi, and E. Molinari, Phys. Rev. B **27**, 1251 (1983).

[7] P. Skeath, C. Y. Su, W. A. Harrison, I. Lindau, and W. E. Spicer, Phys. Rev. B **27**, 6246 (1983).

[8] C. Mailhiot, C. B. Duke, and D. J. Chadi, Phys. Rev. Lett. **53**, 2114 (1984); Phys. Rev. B **31**, 2213 (1985); **31**, 2213 (1985).

[9] John P. LaFemina, C. B. Duke, and C. Mailhiot, J. Vac. Sci. Technol. B **8**, 888 (1990).

[10] A. Tulke, M. Mattern-Klosson, and H. Luth, Solid State Commun. **59**, 303 (1986).

[11] R. M. Feenstra and P. Mårtensson, Phys. Rev. Lett. **61**, 447 (1988).

[12] P. Mårtensson, G. V. Hansson, M. Lahdeniemi, K. O. Magnusson, S. Wiklund, and J. M. Nicholls, Phys. Rev. B **33**, 7399 (1986).

[13] F. Schaffler, R. Ludeke, A. Taleb-Ibrahimi, G. Hughes, and D. Rieger, Phys. Rev. B **36**, 1328 (1987); J. Vac. Sci. Technol. B **5**, 1048 (1987).

[14] W. K. Ford, T. Guo, S. L. Lantz, K. Wan, S. L. Chang, C. B.

Duke, and D. L. Lesser, J. Vac. Sci. Technol. B **8**, 940 (1990).

[15] A. B. McLean, R. Ludeke, M. Prietsch, D. Heskett, D. Tang, and T. M. Wong, Phys. Rev. B **43**, 7243 (1991).

[16] A. Samsavar, M. Prietsch, R. Ludeke (unpublished).

[17] T. Guo, R. E. Atkinson, and W. K. Ford, Rev. Sci. Instrum. **61**, 968 (1989).

[18] C. L. Allyn, T. Gustafsson, and E. W. Plummer, Rev. Sci. Instrum. **49**, 1197 (1978).

[19] D. M. Swanston, A. B. McLean, D. N. McIlroy, D. Heskett, N. J. DiNardo, R. Ludeke, M. Prietsch, and H. Munekata (unpublished).

[20] G. P. Williams, F. Cerrina, G. J. Lapeyre, J. R. Anderson, R. J. Smith, and J. Hermanson, Phys. Rev. B **34**, 5548 (1986).

[21] J. J. Joyce, J. Anderson, M. M. Nelson, and G. J. Lapeyre, Phys. Rev. B **40**, 10 412 (1989).

[22] A number of models were fit to Fig. 2 in order to estimate the mean free path of the photoemitted electrons, the values obtained ranged from 8–15 Å. These are reasonable results for 22-eV photoemitted electrons, which from the universal curve of electron mean free path should have a mean free path of approximately 10 Å.

[23] A fit of a Gaussian distribution to the derivative of the valence edge of a spectrum acquired at normal emission of a clean InAs surface yielded a full width at half maximum of 0.30 eV, which corresponds to an uncertainty in the determination of the VBM of ±0.15 eV.

[24] P. Mårtensson and R. M. Feenstra, Phys. Rev. B **39**, 7744 (1989).

[25] A. M. Bowler, J. C. Hermanson, J. P. La Femina, and C. B. Duke, J. Vac. Sci. Technol. B **10**, 1953 (1992).